

Rapid MIMO-OFDM Software Defined Radio System Prototyping

Amit Gupta, Antonio Forenza, and Robert W. Heath Jr.

Wireless Networking and Communications Group
Department of Electrical and Computer Engineering, The University of Texas at Austin

1 University Station C0803, Austin, TX 78712-0240 USA
Phone: +1-512-232-2014, Fax: +1-512-471-6512
{agupta, forenza, rheath}@ece.utexas.edu

Abstract—Multiple input-multiple output (MIMO) is an attractive technology for future wireless systems. MIMO communication, enabled by the use of multiple transmit and multiple receive antennas, is known for its high spectral efficiency as well as its robustness against fading and interference. Combining MIMO with orthogonal frequency division multiplexing (OFDM), it is possible to significantly reduce receiver complexity as OFDM greatly simplifies equalization at the receiver. MIMO-OFDM is currently being considered for a number of developing wireless standards; consequently, the study of MIMO-OFDM in realistic environments is of great importance. This paper describes an approach for prototyping a MIMO-OFDM system using a flexible software defined radio (SDR) system architecture in conjunction with commercially available hardware. An emphasis on software permits a focus on algorithm and system design issues rather than implementation and hardware configuration. The penalty of this flexibility, however, is that the ease of use comes at the expense of overall throughput. To illustrate the benefits of the proposed architecture, applications to MIMO-OFDM system prototyping and preliminary MIMO channel measurements are presented. A detailed description of the hardware is provided along with downloadable software to reproduce the system.¹

I. INTRODUCTION

Multiple-input multiple-output (MIMO) wireless systems use multiple transmit and multiple receive antennas to increase capacity and provide robustness to fading [1]. To obtain these benefits in broadband channels with extensive frequency selectivity, MIMO communication links require complex space-time equalizers. The complexity of MIMO systems can be reduced, however, through orthogonal frequency division multiplexing (OFDM). OFDM is an attractive digital modulation technique that permits greatly simplified equalization at the receiver. With OFDM, the modulated signal is effectively transmitted in parallel over N orthogonal frequency tones. This converts a wideband frequency selective channel into N narrowband flat fading channels. Currently OFDM is used in many wireless digital communication systems, such as the IEEE 802.11a/g [2], [3] standards for wireless local area networks (WLANs). MIMO-OFDM technology is in the process of being standardized by the IEEE Technical Group 802.11n

[4] and promises to be a strong candidate for fourth generation (4G) wireless communication systems [5].

As the theory behind MIMO-OFDM communication continues to grow, it becomes increasingly important to develop prototypes which can evaluate these theories in real world channel conditions. During the past few years, a number of MIMO-OFDM prototypes have been developed [6]–[12]. These implementations make use of FPGAs or DSPs, which require a large amount of low level programming and a fixed-point implementation. This is the preferred solution when developing high-speed implementations; however, it hinders the flexibility of the platform as these systems are not easily reconfigurable. As a result when experimenting with many different space-time coding schemes or receiver designs, a more flexible solution may be preferred.

In this paper we propose a MIMO-OFDM system architecture based on the software defined radio (SDR) paradigm. The advantage of this approach lies in the fact that the user is not required to have in depth hardware knowledge and may implement a number of different schemes by simply reconfiguring the software. The platform uses National Instruments' radio frequency (RF) hardware in conjunction with the LabVIEW graphical programming language. With this architecture, it is possible to define and simulate a system in a high level programming language and then seamlessly apply that code towards the hardware implementation—this greatly reduces the time involved in system prototyping. Compared with [6]–[12], our prototyping platform can easily be reduplicated as it consists of commercial-off-the-shelf hardware and publicly available software. A user who purchases the RF hardware from National Instruments and downloads the available MIMO software toolkit along with the prototyping code developed by the authors (available at [13], [14]) can realize the same rapid prototyping benefits which we discuss in this paper.

The flexibility of the current implementation of the prototype is limited by some hardware constraints, such as the bandwidth of the PCI bus, which prevents fully real-time transmission over the wireless link, and software constraints like our lack of complete synchronization algorithms in the software, which causes us to use a wired synchronization channel. The spirit of this contribution is to summarize our method and describe our first efforts towards the development

¹This material is based in part upon work supported by the National Instruments Foundation, the National Science Foundation under grant number 0322957, and the Texas Advanced Technology Program under Grant Nos. 003658-0614-2001 and 003658-0380-2003.

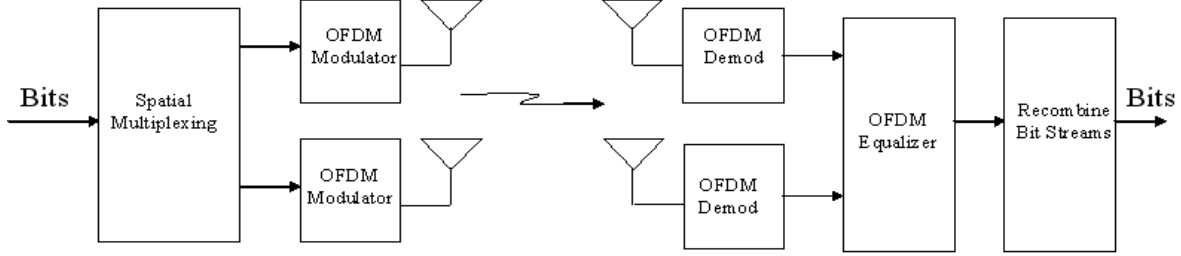


Fig. 1. A 2×2 MIMO-OFDM spatial multiplexing system

of a complete MIMO-OFDM platform designed for system validation and channel measurements. More work needs to be investigated to overcome the limitations and expand the capabilities of our initial design.

This paper is organized as follows. Section II explores the signal model for a MIMO-OFDM system and our specific MIMO-OFDM implementation. Section III discusses the specifics of the hardware and software platform. Section IV shows preliminary results from our system implementation as well as channel measurements in indoor environments.

II. MIMO-OFDM IMPLEMENTATION

In this section we review the MIMO-OFDM signal model and then describe our specific MIMO-OFDM system implementation.

A. MIMO-OFDM Signal Model

In a MIMO-OFDM system (see [8] and the references therein) MIMO space-time codes are combined with OFDM modulation at the transmitter while complicated space-time-frequency processing is employed at the receiver. For simplicity of explanation, we consider spatial multiplexing as illustrated in Fig. 1 though it will be apparent that other transmission techniques can be implemented in the proposed architecture.

In a MIMO-OFDM system with M_T transmit antennas and M_R receive antennas, the sampled signal at the receiver (after the FFT and removing the cyclic prefix) of a spatial multiplexing MIMO system for OFDM symbol period n and tone k can be expressed by the following equation (assuming perfect linearity, timing, and synchronization.) [1]

$$\mathbf{Y}_{n,k} = \mathbf{H}_{n,k} \mathbf{S}_{n,k} + \mathbf{W}_{n,k} \quad (1)$$

where $\mathbf{Y}_{n,k}$ is a $M_R \times 1$ vector representing the M_R received signals, $\mathbf{X}_{n,k}$ is a $M_T \times 1$ vector representing the M_T transmitted signals, $\mathbf{H}_{n,k}$ is the $M_R \times M_T$ MIMO channel matrix that captures the various paths which the signal can travel through from transmitter to receiver, and $\mathbf{W}_{n,k}$ is a vector of complex i.i.d. additive Gaussian white noise.

The channel from transmit antenna t and receive antenna r for the n -th OFDM block and the k -th tone is denoted by

$H_{n,k}^{(r,t)}$ and is computed as

$$H_{n,k}^{(r,t)} = \sum_{\ell=0}^{L-1} h_{n,\ell}^{(r,t)} e^{j \frac{2\pi}{N} \ell k} \quad (2)$$

where $h_{n,\ell}^{(r,t)}$ refers to the time delay profile of the channel and L is the number of channel taps where L must be less than the length of the cyclic prefix to avoid intercarrier interference.

The equalization in MIMO-OFDM systems may be enabled through different procedures such as zero-forcing equalizer, minimum mean-squared error equalizer, V-BLAST successive cancelling equalizer, sphere decoder, and maximum likelihood decoder (see [1] for an overview). In our prototype we currently implement the zero-forcing equalizer; the flexibility of the proposed architecture though allows us to prototype more sophisticated equalization strategies.

B. System Implementation and Specifications

The first implementation features spatial multiplexing with two transmit and two receive antennas, as illustrated in Fig. 1. Other MIMO schemes are already available in the LabVIEW MIMO Toolkit [14], and we are planning to use this to implement other space-frequency codes in the future.

The specifications of the system are listed in Table I. In our MIMO-OFDM implementation, OFDM with 64 tones is employed over a 16MHz bandwidth. The cyclic prefix is 16 samples long. This corresponds to an OFDM symbol duration of $5\mu s$, with a guard interval of $1\mu s$ and a data portion of $4\mu s$. We transmit our OFDM symbols in $200ms$ data packets. This $200ms$ was determined by our hardware as memory constraints at the receiver prevented longer acquisition periods. The system is equipped with an adjustable carrier frequency. We chose to run our system at 2.4GHz, which is the carrier frequency used for WLANs [2], [3]. Various modulation schemes are possible (BPSK, QPSK, 16-QAM, 64-QAM) along with optional convolutional coding.

Channel estimation is carried out by periodically transmitting an OFDM training symbol. The frequency at which training symbols are sent can be programmatically changed in the software and depends on the expected variation of the channel. The estimation at the receiver is enabled by the pilot symbols, sent out over orthogonal tones across the transmit antennas. We then use a linear interpolation across the tones

TABLE I
SPECIFICATIONS OF OUR MIMO-OFDM IMPLEMENTATION

No. of Transmit Antennas	2
No. of Receive Antennas	2
Carrier Freq.	2.4GHz
Bandwidth	16MHz
No. of Tones	64
Subcarrier Spacing	25kHz
OFDM Symbol Duration	5 μ s
Guard Interval Duration	1 μ s
OFDM data duration	4 μ s
Length of Cyclic Prefix	16 samples
MIMO Scheme	spatial multiplexing
Packet Duration	200ms

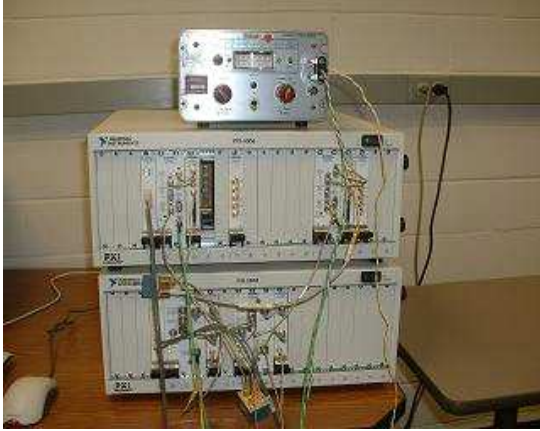


Fig. 2. Picture of the National Instruments RF hardware

to estimate the channel's full frequency response. Once we have a channel estimate, the data is demodulated by a MIMO zero-forcing linear receiver. Due to space limitations, in this contribution we do not provide analytical details of the channel estimation algorithm employed in the prototype.

We are currently avoiding carrier synchronization issues by directly wiring the clocks of the transmitter and receiver together. Additionally, in order to avoid timing issues we are sending a trigger from the transmitter to the receiver when data transmission begins. Software synchronization is under development and will be included in future work.

As we are following a SDR approach to prototyping, there are many parameters of the system which can be adjusted programmatically. The flexibility enabled by a SDR MIMO-OFDM prototype becomes clear in the following section where we present a detailed description of the prototyping platform.

III. PROTOTYPING PLATFORM

A. Hardware Description

National Instruments' RF hardware is the foundation of our prototype, as illustrated in Figure 2. The hardware comes in the PCI extensions for instrumentation (PXI) form factor (which is similar to PCI except designed for industrial applications). Each pair of transmitters and receivers is housed in separate PXI chassis. Each PXI chassis is connected to a PC through a

PCI bridge which connects the PXI hardware to the PCI bus. Each PC is equipped with dual 2.8GHz processors and 2Gb of memory. The specifications of the hardware is listed in Table II and the corresponding block diagram is depicted in Figure 3.

TABLE II
HARDWARE SPECIFICATIONS

Transmitter	Arbitrary Waveform Generator PXI-5421	100 million samples per sec. 16 bit resolution 43MHz bandwidth
	Upconverter PXI-5610	250KHz - 2.7GHz Carrier +13dB range
	Receiver	
Receiver	Digitizer PXI-5620	64 million samples per sec. 14 bit resolution 30MHz bandwidth
	Downconverter PXI-5600	9kHz - 2.7GHz Carrier 20MHz real-time bandwidth

Each transmit unit is called a RF signal generator and it consists of two parts. The first is the arbitrary waveform generator (ARB). The ARB acts as the digital to analog converter (DAC) and it operates at a maximum of 100M samples/sec with a 16-bit resolution. The ARB has a 256MB buffer, although the hardware is enabled to cycle through the buffer to provide for continuous transmission. When transmitting complex data, the ARB itself upconverts the signal to an intermediate frequency (IF) of 25MHz (this IF can be programmatically changed) before the signal is sent to the RF upconverter. The upconverter can modulate a signal up to a carrier frequency of 2.7GHz with bandwidths up to 20MHz and is capable of a maximum of 13dBm of power. The ARB has a trigger line available for timing synchronization, while the upconverter has an input available for clock synchronization.

The receiver also consists of two units: a digitizer and a RF downconverter. The downconverter takes the RF signal from the antenna and downconverts it to an IF frequency of 15MHz before sending it to the digitizer (A/D). Like the upconverter, the downconverter can process signals up to 2.7GHz. The downconverter can process 20MHz bandwidth blocks of data at a time. The digitizer runs at a maximum sampling rate of 64Msamples/sec and it has a 14-bit resolution. It is equipped with a 64MB buffer. The digitizer samples the IF waveform and sends it to the PC where IF demodulation happens in software. This software demodulation along with the limited speed of the PCI bus prevents continuous operation at maximum bandwidth. Using a duty cycle (transmitting a only a fraction of every cycle) allows us to transmit using large bandwidths while decreasing the bandwidth below 1.25MHz (where onboard digital demodulation is supported) allows us to support continuous streaming.

To extend the usable range of the prototype we used a Mini-circuits ZQL-2700MLNW LNA (low noise amplifier) at the receiver. We derived the gain of the LNA from the link-budget equation [15]

$$P_R = P_T + G_T + G_R - PL - L_c + G_{LNA} \quad (3)$$

where P_T and P_R are the transmitter and receiver powers

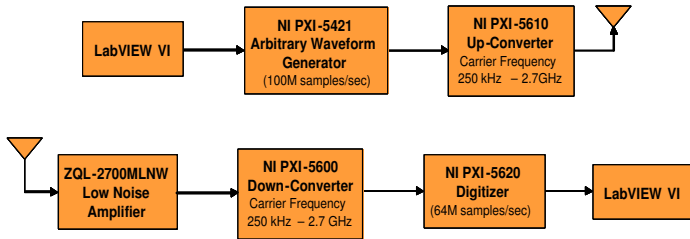


Fig. 3. Hardware block diagram

in dBm, $G_T = G_R = 3\text{dB}$ are the transmitter and receiver antenna gains, $PL = 60\text{dB}$ is the path-loss at 2.4GHz calculated for 20 meter range between transmitter and receiver, $L_c = 15\text{dB}$ is the loss due to the cables used to connect the antennas to the PXI chassis. According to (3), we found that a gain of $G_{LNA} = 25\text{dB}$ is required for the LNA in order to guarantee a minimum received power of approximately $P_R = -40\text{dBm}$, when the transmit power is set to $P_T = 5\text{dBm}$.

Additionally, for timing and clock synchronization, we found that we needed a 3 way power splitter to send each signal out to each of the transmit and receive components. This splitter will be replaced once full open loop synchronization is implemented.

B. Software Description

The RF Hardware is designed to be easily configured and programmed through National Instruments' LabVIEW programming environment. LabVIEW is a data flow based graphical programming language. The hardware can be programmed in other languages, however, LabVIEW provides the user with simple programming and rapid prototyping capabilities. We began the prototyping process by creating a simulation of the MIMO-OFDM system in LabVIEW. For this purpose our research group has created a publicly available MIMO toolkit for LabVIEW which can be downloaded at [14]. This toolkit includes the building blocks to simulate various MIMO schemes as well as the functions which are necessary to simulate the system completely from baseband up to the modulation and decoders. The MIMO schemes that are currently included in the toolkit are spatial multiplexing, Alamouti encoding, linear dispersion encoding, trellis coding, along with other common MIMO schemes and functions to support simulation.

After completing simulations, the next stage in our prototyping process was to actually program the hardware. With the LabVIEW simulations already completed, the transition to hardware programming was very simple as the code written for the system simulation could then be applied with the hardware. Many of the low level hardware issues were avoided by using the LabVIEW hardware device drivers.

IV. RESULTS

In this section we describe a simple system implementation as well as a basic channel measurement setup. Both imple-

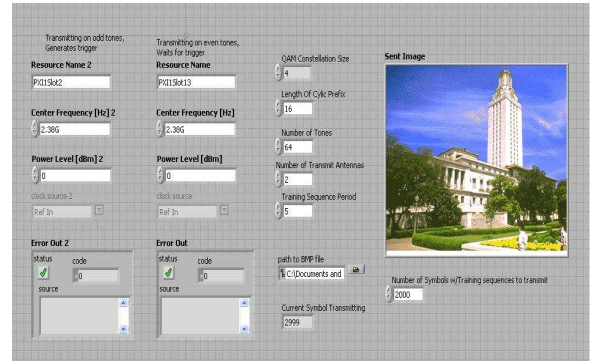


Fig. 4. The LabVIEW transmitter software interface with various programmable system parameters

mentations are available for download at [13] along with the MIMO Toolkit [14].

A. MIMO-OFDM System Implementation

One of the objectives of hardware implementation was to test various candidate coding and receiver strategies for the MIMO-OFDM physical layer under consideration in the IEEE 802.11n standard, which is currently under development. The system followed the specifications outlined in Section III with a 2×2 spatial multiplexing MIMO system combined with 64 OFDM tones. QPSK modulation was combined with a channel estimation scheme that sends a training symbol every fifth OFDM symbol. As previously discussed, due to memory constraints, only 200ms worth of packets of data are transmitted in a given time interval. In this period we are consistently able to achieve a data rate of 40.96 Mbits/s (8.192 Mbits are transmitted in this 200ms time frame) with our given hardware.

Due to our current hardware limitations, each acquisition requires approximately 4 seconds of processing before a new acquisition can occur. Thus the overall throughput we achieve is about 2 Mbits when operated using this duty cycle. Future hardware upgrades will allow real time system implementations.

For demonstration purposes we transmitted an image as displayed in the graphical user interface (GUI) depicted in Figure 4. The decoded image is reported in Figure 5 along with the GUI at the receiver side. The difference in download speed of the image in non-MIMO and MIMO configurations provides an intuitive motivation for MIMO, e.g. the image transfers twice as fast with MIMO in our configuration.

We will continue to build on our current system implementation as we implement a number of other available MIMO schemes which are available through our MIMO toolkit [14]. We are also investigating adding a medium access control (MAC) protocol as well as a feedback channel.

B. Channel Measurements

Along with the system implementation, we are using the prototype to conduct channel measurements. We only have

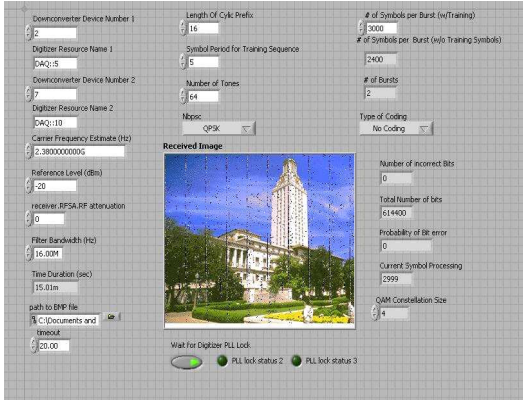


Fig. 5. The LabVIEW receiver software interface with various programmable system parameters.

preliminary results from the hardware, but they reveal the potential of this approach for conducting meaningful channel measurements. We performed the channel measurements in the wireless networking and communications group’s (WNCG) workspace in the Engineering Science building at The University of Texas at Austin. The environment is a typical cubicle office environment. We collected data at a carrier frequency of 2.4GHz over a 16MHz bandwidth with 64 tones. We employed half-wavelength omnidirectional dipole antennas for our channel measurements to radiate isotropically along multiple propagation paths, distributed around transmitter and receiver according to the model in [16]. The transmit and receive antennas were placed approximately 8 meters apart in between cubicles so that there was no line of sight propagation paths, with two walls between the transmitter and receiver. The two transmit antennas were spaced five wavelengths apart from each other (approximately 60 centimeters) to reduce the spatial correlation across different MIMO channels [17] and the effect of mutual coupling [18]. The two receive antennas were separated by the same distance.

We measured the MIMO channels over the time and frequency domains and the results are shown in Figure 6. The temporal evolution of the channel is flat due to the low Doppler effect in fixed wireless scenarios, whereas the fluctuations in the frequency domain are due to the multiple propagation paths.

In Figure 7 we display the average power delay profile (PDP) of channel H_{22} . We found a good fit of this PDP with well known models and measurements results for indoor propagation environments [12], [16], [19]. Note that the modest selectivity of the channel H_{22} is due to the small spread in the delay profile.

V. CONCLUSIONS AND FUTURE WORK

In this paper, we presented a MIMO-OFDM prototyping architecture which emphasizes a SDR paradigm. The platform frees the user from low-level hardware implementation issues and allows more intensive study of algorithm and system design issues. We illustrated applications of this approach to

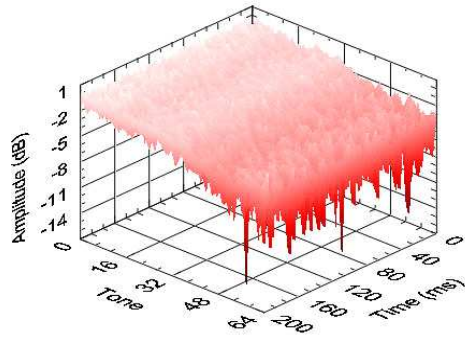
system implementation and channel measurements. In future work we plan to apply this to study MAC protocol designs for MIMO-OFDM ad hoc networks [22] as well as to more comprehensively analyze MIMO channels as in [21].

ACKNOWLEDGEMENTS

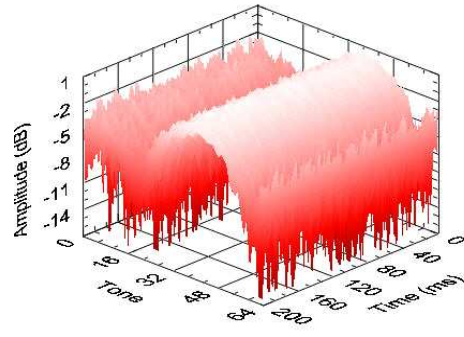
The authors would like to thank National Instruments for their hardware donation as well as Andy Hinde at National Instruments for his assistance with the hardware and UT Austin students Brett Westervelt and Veynu Narasiman for their contributions to the system prototype.

REFERENCES

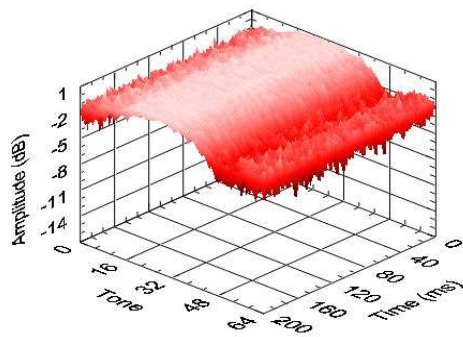
- [1] A. Paulraj, R. Nabar, and D. Gore, *Introduction to Space-Time Wireless Communications*. Cambridge University Press, 2003.
- [2] “Part 11: Wireless LAN Medium Access Control (MAC) and Physical Layer (PHY) Specifications: High-Speed Physical Layer in the 5 GHz Band,” IEEE Standard 802.11a 1999.
- [3] “Part 11: Wireless LAN Medium Access Control (MAC) and Physical Layer (PHY) specifications Amendment 4: Further Higher-Speed Physical Layer Extension in the 2.4 GHz Band,” IEEE Standard 802.11g 2003.
- [4] “IEEE 802.11n Task Group,” http://grouper.ieee.org/groups/802/11/Reports/tgn_update.htm.
- [5] H. Sampath, S. Talwar, J. Tellado, V. Erceg, and A. Paulraj, “A Fourth-Generation MIMO-OFDM Broadband Wireless System: Design, Performance, and Field Trial Results,” *IEEE Communications Magazine*, vol. 40, no. 9, pp. 143–149, September 2002.
- [6] A. Adjoudani et. al., “Prototype Experience for MIMO BLAST over Third-Generation Wireless System,” *IEEE Journal on Selected Areas in Comm.*, vol. 21, no. 3, pp. 440–451, April 2003.
- [7] P. Murphy, F. Lou, and P. Frantz, “A Hardware Testbed for the Implementation and Evaluation of MIMO Algorithms,” in *IEEE International Conference on Mobile and Wireless Communications Networks*, October 2003.
- [8] G. L. Stuber, J. R. Barry, S. W. Mclaughlin, Y. Li, M. A. Ingram, and T. G. Pratt, “Broadband MIMO-OFDM Wireless Communications,” in *Proc. of the IEEE*, Feb. 2004, vol. 92, pp. 271–294.
- [9] T. Sugiyama, S. Kurosaki, Y. Asai, and M. Umehira, “Development of a Novel SDM-COFDM Prototype for Broadband Wireless Access Systems,” in *Wireless Communications and Networking Conference*, March 2003, vol. 1, pp. 55–61.
- [10] S. H. Won, Deuk-Su Lyu, and H. J. Park, “Physical Layer Implementation and Evaluation of Multiple Input Multiple Output-Orthogonal Frequency Division Multiplexing (MIMO-OFDM) System,” in *Proceedings of the ICCT*, April 2003, vol. 2, pp. 1384–1352.
- [11] A. van Zelst and T. C. W. Schenk, “Implementation of a MIMO OFDM-based Wireless LAN System,” *IEEE Trans. on Signal Processing*, vol. 52, no. 2, pp. 483–494, Feb. 2004.
- [12] Univ. of Southern California Ultra Lab, “Intel UWB and MIMO Channel Measurement Database,” <http://impulse.usc.edu/>.
- [13] A. Gupta and R. W. Heath Jr., “MIMO-OFDM Prototyping Code for LabVIEW,” <http://www.ece.utexas.edu/rheath/research/mimo/proto/>.
- [14] S. Patil and R. W. Heath Jr., “LabVIEW MIMO Toolkit,” <http://www.ece.utexas.edu/rheath/research/mimo/toolkit.php>.
- [15] G. Durgin, T. S. Rappaport, and Hao Xu, “Measurements and models for radio path loss and penetration loss in and around homes and trees at 5.85 GHz,” *IEEE Transactions on Communications*, vol. 46, pp. 1484 – 1496, November 1998.
- [16] V. Erceg et. al., “TGN channel models,” *IEEE 802.11-03/940r4*, <http://www.802wirelessworld.com:8802/>, May 2004.
- [17] A. Foreza and R. W. Heath Jr., “Impact of Antenna Geometry on MIMO Communication in Indoor Clustered Channels,” to appear on *IEEE APS-IS’04*, June 2004.
- [18] J. W. Wallace and M. A. Jensen, “Termination-dependent diversity performance of coupled antennas: Network theory analysis,” *IEEE Transactions on Antennas and Propagation*, vol. 52, pp. 98 – 105, Jan. 2004.
- [19] A. A. M. Saleh and R. A. Valenzuela, “A statistical model for indoor multipath propagation,” *IEEE Journal on Selected Areas in Communications*, vol. SAC-5, no. 2, pp. 128–137, February 1987.



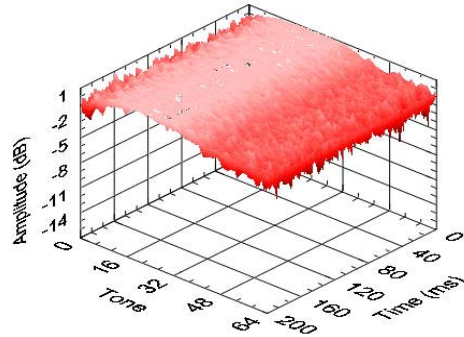
(a) Channel $H^{(1,1)}$



(b) Channel $H^{(1,2)}$



(c) Channel $H^{(2,1)}$



(d) Channel $H^{(2,2)}$

Fig. 6. MIMO channel frequency response for different channels.

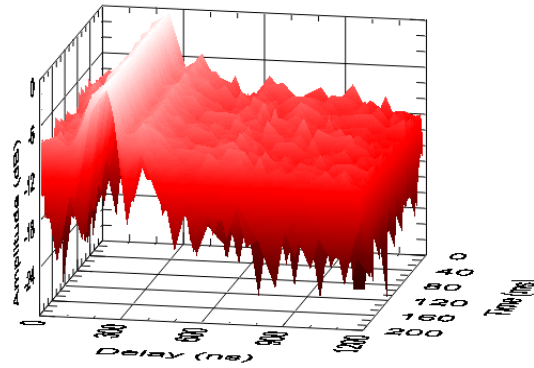
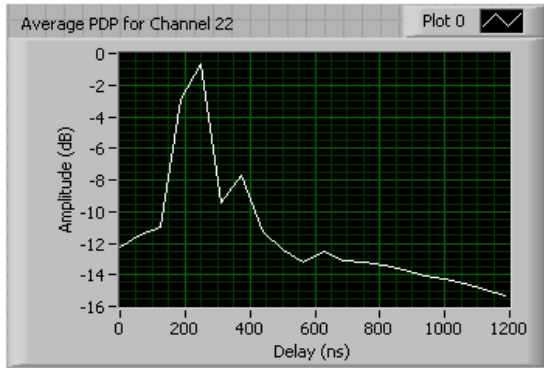


Fig. 7. Power delay profile (PDP) of Channel $H^{(2,2)}$ in 2D and 3D.

[20] T. Tang, M. Park, Jr. R. W. Heath, and S. M. Nettles, "A Joint MIMO-OFDM Transceiver and MAC Design for Mobile Ad Hoc Networking," in *Proceedings of the International Workshop on Wireless Ad Hoc Networks*, Oulu, Finland, May 31 - June 3 2004.

[21] J. W. Wallace, M. A. Jensen, A. L. Swindlehurst, and B. D. Jeffs, "Experimental characterization of the MIMO wireless channel: data acquisition and analysis," *IEEE Transactions on Wireless Communications*, vol. 2, pp. 335 - 343, March 2003.